

572

PHYSICAL REVIEW B

CONDENSED MATTER

THIRD SERIES, VOLUME 41, NUMBER 6

15 FEBRUARY 1990-II

Theory of spin-polarized metastable-atom-deexcitation spectroscopy: Ni-He

David R. Penn

Radiation Physics Division, National Institute of Standards and Technology, Gaithersburg, Maryland 20899

Peter Apell

Institute for Theoretical Physics, University of Umeå, S-901 87 Umeå, Sweden

(Received 21 August 1989)

Metastable spin-polarized He^* atoms incident on a Ni surface undergo deexcitation in a process which yields electrons from the Ni. The number produced is observed to depend on the relative spin of the Ni and the He^* atoms. The normalized difference in the ejected-electron intensity produced by He^* atoms with opposite spin polarizations increases dramatically with increasing kinetic energy of the electrons. A theory of this asymmetry is presented. It is found that the experimental results can be reproduced only by the use of a realistic potential for the Ni electrons in the vacuum region. With such a potential it is found that He^+ ions which result from the He^* -surface interaction are neutralized at $\sim 4.5 \text{ \AA}$ from the Ni surface, a much larger distance than given by previous estimates. The experiment is shown to reflect the polarization of Ni electrons at the He ion, and it is estimated that the Ni magnetization at the Fermi energy and far from the Ni surface is $\approx -20\%$.

I. INTRODUCTION

There has been increasing interest in the spin-dependent properties of magnetic solids over the last decade.^{1,2} In particular, the spin dependence of electron scattering from surfaces³⁻⁵ and the polarization of secondary electrons in magnetic transition metals and related ferromagnetic metallic glasses⁶⁻¹¹ has been studied in detail. One aim in such studies has been to probe the elementary excitation spectrum of the magnetic material, i.e., spin waves and Stoner excitations. Whereas the former has been investigated extensively with use of neutron scattering,¹² only recently have techniques been developed to study the single-particle excitations.^{3-5,13-15} The most recent of these experiments¹⁴ utilizes a spin-polarized beam as well as spin detection of the scattered electrons to obtain information about four scattering channels. Other spin-sensitive probes include spin-polarized inverse photoelectron spectroscopy,^{15,16} spin-polarized photoemission,¹⁷⁻²² spin-polarized Auger-electron spectroscopy,²³⁻²⁵ spin-resolved tunneling from ferromagnetic materials,²⁶⁻²⁹ spin-polarized low-energy electron diffraction (LEED),^{30,31} electron-capture spectroscopy,³²⁻³⁴ and spin-polarized positron spectroscopy.³⁵

The probe dealt with in this paper is spin-polarized metastable-atom-deexcitation spectroscopy^{2,36} (SPMDS). In this technique a thermal beam of metastable $\text{He}(2^3S)$

atoms is electron-spin polarized by optical pumping and is then directed at the surface under study. The spin-polarized atoms are deexcited when they interact with the surface and electron emission from the metal results. As is well known from the many previous investigations that utilized unpolarized metastable atoms,³⁷⁻⁵⁰ this technique provides the opportunity to study surface and adsorbate electronic structure with extreme surface specificity. With the addition of spin polarization, this technique can be used to study surface magnetism³⁶ as well as the dynamics of metastable-atom-surface interactions.³⁷

In the experiment under consideration,³⁶ electron-spin-polarized atoms are directed at a clean magnetized Ni(110) surface. The atoms are polarized either parallel or antiparallel to the magnetization of the sample. As the $\text{He}(2^3S)$ atoms approach the surface they resonantly ionize as the excited $2s$ electron tunnels into an empty state above the Fermi level. The resulting He^+ ion is subsequently neutralized by a conduction electron from the surface which fills the He $1s$ hole in an Auger-like process in which a second Ni electron is ejected. This process, Auger neutralization, plays a key role in the closely related technique of ion neutralization spectroscopy.⁵¹⁻⁶²

Since the incident $\text{He}(2^3S)$ atoms are electron-spin polarized in a selected direction, the spin of the electron which fills the He^+ $1s$ hole is known. For a given in-

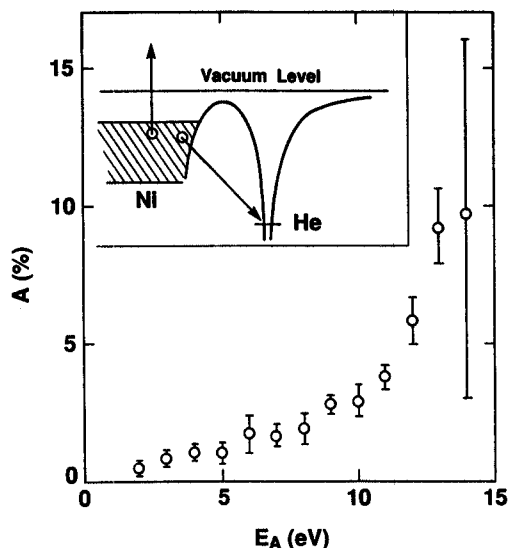


FIG. 1. The experimental integrated normalized spin asymmetry, $A^>$, as a function of energy E_A (from Ref. 36). The inset illustrates the neutralization of a He^+ ion by an Auger-like process. A Ni electron spin σ fills the empty $1s$ σ state of the He^+ ion and a second Ni with energy E_A is excited.

cident spin direction, all electrons ejected from the Ni surface with an energy greater than some energy E_A are collected, regardless of spin. The number collected is $N_{\downarrow}^>(E_A)$, where \downarrow refers to the spin of the Ni electron that fills the He $1s$ state. The spin of the He atoms is reversed and again all ejected Auger electrons with energy greater than E_A are collected. The integrated normalized spin asymmetry is defined as

$$A^>(E_A) = \frac{N_{\downarrow}^>(E_A) - N_{\uparrow}^>(E_A)}{N_{\downarrow}^>(E_A) + N_{\uparrow}^>(E_A)}. \quad (1)$$

The experimental results for $A^>(E_A)$ are shown in Fig. 1. The purpose of this paper is to report on calculations of the asymmetry, $A^>(E_A)$, and to understand what properties of the Ni are measured in SPMDS.

Section II is a discussion of the model on which our calculations are based. Section III gives the general theory for SPMDS. In Sec. IV the Auger rates are discussed, and in Sec. V the numerical results are presented. The conclusions are given in Sec. VI.

II. MODEL FOR SPMDS CALCULATIONS

In Ref. 36 a thermal beam of metastable spin-polarized He is incident on a clean Ni(110) surface. Figure 2 shows the relevant energies. The $\text{He}^*(2^3S)$ level is 4.77 eV below the vacuum level; i.e., the ionization energy of $\text{He}^*(2^3S)$ is 4.77 eV. The ionization energy of neutral He in its ground state, E^0 , is 24.6 eV. Both of these values are for an isolated atom. At a distance z from a metal surface the screening of an ionized He atom will lower the ionization energy by an amount given by the image-potential shift, $e^2/4z$. The Ni(110) work function is 5.04 eV.⁶³ There are⁶⁴ approximately 4.7 majority spin d elec-

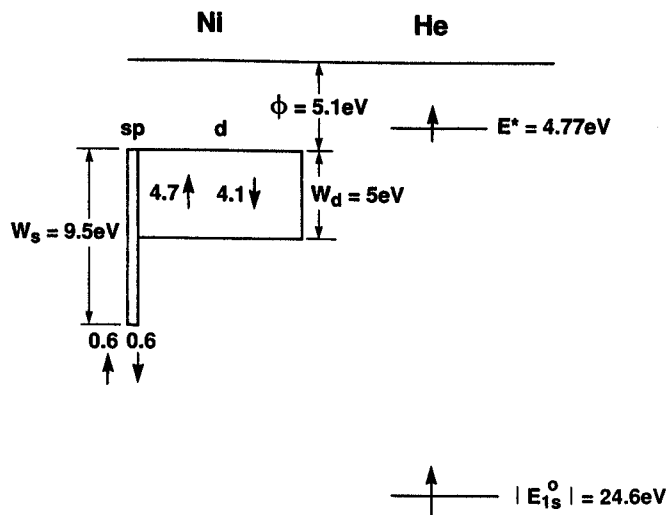


FIG. 2. Summary of relevant energies and electron occupation numbers for the metastable He-Ni system.

trons (spin \uparrow) and 4.1 minority spin electrons (spin \downarrow) in a band approximately 5 eV wide. There are approximately an equal number of spin \uparrow and spin \downarrow s - p electrons, $n_s = 0.6$, in a band of width 9.5 eV. In the surface region the d band narrows to roughly 3 eV.⁶⁵

Experiments⁶⁶ from metals with work functions greater than the $\text{He}^*(2^3S)$ ionization energy have shown that the metastable He^* atoms are resonantly ionized with almost unit probability. This resonant ionization occurs when the excited $2s$ electron of the He^* atom tunnels into the empty s - p states of the metal. It takes place in the range 5–10 Å from the metal surface where the $2s$ He^* wave function starts to overlap the metal surface atoms. In the region < 5 Å there is subsequent neutralization of the He^+ ion via an Auger-like transition in which a metal electron fills the empty He $1s$ state and a metal Auger electron is ejected. Thus the Auger spectra produced by incident He^* atoms are virtually identical with that produced by He^+ ions and the starting point of the paper is the calculation of the Auger neutralization of spin-polarized He^+ ions.

A rough description of the neutralization is given by the theories of Cobas and Lamb,⁵⁸ Hagstrum,⁵¹ and others,⁶¹ who derive a most probable distance for the neutralization. Far from the solid there is a low filling probability for the He $1s$ level, often written as $R = R_0 e^{-\gamma z}$, where z is distance to the surface and $1/\gamma$ is associated with the exponential decrease of the metal wave function in the vacuum region. The number of empty $1s$ levels, $n(z)$, at a distance z from the surface is given by $dn/dt = -Rn$.

The solution of the rate equation is

$$n(z) = \exp \left[- \int_z^\infty dz' \Gamma(z') \right], \quad (2)$$

where (note: $v = -\partial z / \partial t$)

$$\Gamma(z) = R(z)/v(z) \quad (3)$$

and the probability that the He $1s$ level is filled at a dis-

tance z is $P = Rn/v$, where^{ff}

$$P(z) = \Gamma(z) \exp \left[- \int_z^\infty dz' \Gamma(z') \right]. \quad (4)$$

The maximum of $P(z)$ occurs at $z = z_m$, where

$$0 = \frac{\partial \Gamma}{\partial z} \bigg|_{z=z_m} + \Gamma^2(z_m) \quad (5)$$

or

$$z_m = \frac{1}{\gamma} \ln \left[\frac{R_0}{v \left[\gamma + \frac{1}{v} \frac{\partial v}{\partial z} \right]} \right]. \quad (6)$$

The velocity v is determined by the image potential

$$\frac{1}{2} M v^2(z) = \frac{e^2}{4z} + E_{\text{inc}}, \quad (7)$$

where E_{inc} is the incident energy of the thermal He atoms and M is the mass of the He atom. In Eq. (6) the quantity γ can be estimated by $2(2m\phi/\hbar^2)^{1/2}$, where ϕ is the Ni work function. Equation (6) then yields a value of $z_m = 1 \text{ \AA}$, 1.5 \AA , and 2 \AA for $R_0 = 1.4 \times 10^{15} \text{ s}^{-1}$, $2.7 \times 10^{15} \text{ s}^{-1}$, and $8.7 \times 10^{15} \text{ s}^{-1}$, where R_0 is defined by $R(z) = R_0 e^{-\gamma z}$.

Our calculation of the SPMDS experiment of Ref. 36 is based on the following picture. A metastable He* atom with a definite polarization (say \uparrow) corresponding to a hole in the $1s \downarrow$ level approaches the Ni surface and resonantly ionizes leaving a He⁺ ion with a $1s \downarrow$ hole. The He⁺ ion is subsequently Auger neutralized and a Ni Auger electron is produced. For every incident He* atom, regardless of its spin, one Auger electron is produced and the integrated asymmetry is zero. If only those electrons with energy greater than say E_A are collected, then a nonzero integrated asymmetry $A^>(E_A)$ is measured. The larger E_A the greater the asymmetry for E_A up to a maximum value E_A^0 :

$$E_A^0 = |E_{1s}^0| - 2\phi, \quad (8)$$

where ϕ is the work function and E_{1s}^0 is the energy of the empty He $1s$ level when the He is far from the surface. The zero of energy is taken to be the vacuum level. The term 2ϕ in Eq. (8) arises because the two metal electrons involved in the Auger process must originate at the Fermi level if the maximum Auger energy is to be produced. As the He⁺ ion approaches the surface the maximum Auger energy at which electrons are produced decreases due to the change in the He $1s$ energy, $E_{1s}(z)$, which is affected by the image potential. The maximum Auger energy for a given z is

$$E_A^{\text{max}}(z) = |E_{1s}(z)| - 2\phi. \quad (9)$$

For a value of E_A (less than E_A^0), only Auger transitions that take place farther from the surface than $z_{\text{min}}(E_A)$ will be observed where

$$E_A = |E_{1s}(z_{\text{min}})| - 2\phi \quad (10)$$

determines z_{min} . For $z < z_{\text{min}}$ all Auger transitions will produce electrons at energies less than E_A . For $E_A \approx E_A^0$ only transitions far from the surface can be observed. If the He $1s \downarrow$ holes are filled more rapidly than the He $1s \uparrow$ holes, then a positive asymmetry will be observed, $A^>(E_A) > 0$. It will be seen that He $1s \downarrow$ holes fill faster than $1s \uparrow$ holes because there are more metal spin \downarrow electrons than spin \uparrow electrons in the vacuum region corresponding to a negative spin polarization.

For a smaller value of E_A there is a smaller value of z_{min} and Auger transitions that take place closer to the surface also contribute to the observed spectrum. By the time it gets near the surface a He⁺ ion that began with a $1s \downarrow$ hole is more likely to have filled than a $1s \uparrow$ hole. This means that near the surface there is a greater probability for the filling of a He $1s \uparrow$ hole than for a He $1s \downarrow$ hole even though the filling rate is largest for \downarrow holes, i.e., filling probability is equal to rate times number of holes available. This implies a reduction in the asymmetry. In the limit that E_A is reduced to the point where all Auger electrons are collected, $A^> = 0$.

III. THEORY

A theory of the asymmetry measured in SPMDS is developed in this section. Let $r_\sigma(E_A, z)$ be the rate per unit energy that Ni Auger electrons of either spin are produced at energy E_A by a He⁺ ion located a distance z from the surface with a spin σ hole in its $1s$ shell. Such a He⁺ ion is said to be polarized in the spin $\bar{\sigma}$ direction (where $\bar{\sigma}$ is opposite to σ) due to the electron in the $1s\bar{\sigma}$ state. Let $n_\sigma(z)$ be the probability that the initially empty $1s \sigma$ hole is still empty after the ion, initially at $z = \infty$, has reached a distance z from the surface. The number of Auger electrons per unit energy produced with energy E_A by an incident He⁺ ion is

$$N_\sigma(E_A) = \int_0^\infty \frac{dz}{v(z)} r_\sigma(E_A, z) n_\sigma(z), \quad (11)$$

where $v(z) = -dz/dt$ is the velocity of the He atom. Far from the surface $n_\sigma(z) \rightarrow 1$ and $n_\sigma(z)$ decreases monotonically with decreasing z . In order to determine $n_\sigma(z)$ we use the rate equation $(dn/dt) = -Rn$, i.e.,

$$\frac{d}{dz} n_\sigma(z) = \frac{R_\sigma(z)}{v(z)} n_\sigma(z), \quad (12)$$

where $R_\sigma(z)$ is the total rate at which Auger electrons are produced by a He $1s \sigma$ hole at distance z from the surface

$$R_\sigma(z) = \int_{-\infty}^\infty dE_A r_\sigma(E_A, z). \quad (13)$$

Equation (12) has the solution

$$n_\sigma(z) = \exp \left[- \int_z^\infty dz' [R_\sigma(z')/v(z')] \right]. \quad (14)$$

Thus a knowledge of the rate at which Auger electrons are produced, $r_\sigma(E_A, z)$, yields the number of Auger electrons per unit energy produced at energy E_A , $N_\sigma(E_A)$, by a He⁺ ion with a $1s \sigma$ hole incident on a Ni surface. The quantity $N_\sigma(E_A)$ obeys a sum rule

$$Y_\sigma = \int_{-\infty}^{\infty} dE_A N_\sigma(E_A) = 1 - n_\sigma(z=0) \quad (15)$$

which follows directly from Eqs. (11)–(13). In Eq. (15), Y_σ is the yield (the total number of Auger electrons) for a He^+ ion with a $1s$ hole of spin σ . In practice $n_\sigma(z=0) \ll 1$ and the yield is essentially unity. A He^+ atom with a $1s$ hole incident on a surface will produce one Auger electron due to the filling of the $1s$ hole. The actual measured yield is smaller than 1 because not all Auger electrons escape into the vacuum. However, the escape probability will depend only on energy and not on spin so that $A^>(E_A)$ is not effected. We therefore neglect the escape probability in this paper.

The asymmetry for Auger electrons of kinetic energy E_A is

$$a(E_A) = N_\downarrow(E_A) - N_\uparrow(E_A). \quad (16)$$

Equation (15) requires

$$\int_{E_A^{\min}}^{E_A^{\max}} dE_A a(E_A) \approx 0, \quad (17)$$

where E_A^{\min}, E_A^{\max} are the minimum and maximum energies at which Auger electrons are produced. The energy E_A will be measured from the vacuum level. Thus the lowest value of E_A that can be observed is $E_A = 0.0$, however $A^>(0.0)$ need not be zero since $E_A^{\min} < 0.0$. Those electrons with $E_A < 0.0$ cannot be observed. The normalized asymmetry is $a(E_A) / [N_\downarrow(E_A) + N_\uparrow(E_A)]$. The Ni SPMDS experiment measures an integrated normalized asymmetry given by

$$A^>(E_A) = \frac{N_\downarrow^>(E_A) - N_\uparrow^>(E_A)}{N_\downarrow^>(E_A) + N_\uparrow^>(E_A)}, \quad (18)$$

where $N_\sigma^>(E_A)$ is the number of Auger electrons with energy greater than or equal to E_A :

$$N_\sigma^>(E_A) = \int_{E_A}^{\infty} dE N_\sigma(E). \quad (19)$$

From (17) it follows that $A^>(E_A^{\min}) \approx 0$.

In order to calculate $A^>(E_A)$, define

$$r_\uparrow(E_A, z) = r_0(E_A, z) + \Delta r(E_A, z), \quad (20)$$

$$r_\downarrow(E_A, z) = r_0(E_A, z) - \Delta r(E_A, z). \quad (21)$$

It will be shown in Sec. IV that $\Delta r/r_0$ is related to the polarization which is small in Ni.

The rates $R_0(z), \Delta R(z)$ are defined by

$$R_0(z) = \int_{-\infty}^{\infty} dE_A r_0(E_A, z), \quad (22)$$

$$\Delta R(z) = \int_{-\infty}^{\infty} dE_A \Delta r(E_A, z), \quad (23)$$

in analogy with Eq. (13). Similarly, n_0 and Δn are defined by

$$n_\uparrow = n_0 + \Delta n, \quad (24)$$

$$n_\downarrow = n_0 - \Delta n. \quad (25)$$

Use of Eqs. (20)–(25) in Eqs. (13) and (14) yields

$$n_0(z) = \exp \left[- \int_z^{\infty} dz' R_0(z') / v(z') \right], \quad (26)$$

$$\Delta n(z) = -n_0(z) \int_z^{\infty} dz' \Delta R(z') / v(z'), \quad (27)$$

to lowest order in ΔR . The asymmetry $a(E_A)$ of Eq. (16) is given to lowest order by

$$a(E_A) = -2 \int_0^{\infty} dz \frac{1}{v(z)} n_0(z) \left[\Delta r(E_A, z) - r_0(E_A, z) \int_z^{\infty} dz' \frac{1}{v(z')} \Delta R(z') \right], \quad (28)$$

which follows from Eqs. (16), (24), (25), and (27). The total number of Auger electrons at energy E_A is

$$N(E_A) \equiv N_\uparrow(E_A) + N_\downarrow(E_A) = 2 \int_0^{\infty} dz \frac{1}{v(z)} n_0(z) r_0(E_A, z). \quad (29)$$

The first term on the right-hand side of Eq. (28) represents the contribution to the asymmetry due to the difference in the rates at which He^+ ions of different spin produce Auger electrons. The second term on the right-hand side of Eq. (28) takes into account the difference in availability of He^+ holes of different spin. It is easy to show that $a(E_A)$ given by Eq. (28) satisfies the sum rule Eq. (17).

The expression for $a(E_A)$ given by Eq. (28) can be rewritten as

$$a(E_A) = -2 \int_0^{\infty} dz P_0(z) \left[\Delta I(E_A, z) \varphi(z) - I(E_A, z) \int_z^{\infty} dz' \frac{1}{v(z')} R_0(z') \varphi(z') \right], \quad (30)$$

where

$$P_0(z) = \frac{n_0(z) R_0(z)}{v(z)}, \quad (31)$$

$$\Delta I(E_A, z) = \frac{\Delta r(E_A, z)}{\Delta R(z)}, \quad (32)$$

$$I(E_A, z) = \frac{r_0(E_A, z)}{R_0(z)}, \quad (33)$$

$$\varphi(z) = \frac{\Delta R(z)}{R_0(z)}. \quad (34)$$

In Eq. (30), $P_0(z)$ is the probability of neutralization at a distance z . The quantities $\Delta I(E_A, z)$ and $I(E_A, z)$ are the normalized Auger distributions corresponding to the

difference and the sum of the Auger production rates $r_{\uparrow}(E_A, z)$ and $r_{\downarrow}(E_A, z)$:

$$\int_{-\infty}^{\infty} dE_A \Delta I(E_A, z) = 1, \quad (35)$$

$$\int_{-\infty}^{\infty} dE_A I(E_A, z) = 1. \quad (36)$$

The quantity $\varphi(z)$ is the ratio of the difference to the sum of Auger production rates at a metal-He separation z . Just as in Eq. (28), the first term on the right-hand side of Eq. (30) describes the asymmetry produced by the difference in the rates $r_{\uparrow}(E_A, z)$ and $r_{\downarrow}(E_A, z)$. The second term arises because as the He^+ gets closer to the surface there is a lower probability of (say) a spin \downarrow being available for filling due to the fact that they fill more rapidly than spin \uparrow holes corresponding to $\Delta r = r_{\uparrow} - r_{\downarrow} < 0$.

Similarly, Eq. (29) can be written

$$N(E_A) = 2 \int_0^{\infty} dz P_0(z) I(E_A, z). \quad (37)$$

In the case where $\varphi(z)$ is independent of z , Eq. (30) simplifies to

$$\varphi(z) = \bar{\varphi} = \text{const}, \quad (38)$$

$$a(E_A) = -2\bar{\varphi} \int dn_0 [\Delta I(E_A, z) + I(E_A, z) \ln n_0], \quad (39)$$

where use has been made of the relation

$$\frac{d}{dz} n_0(z) = P_0(z) \quad (40)$$

and $z = z(n_0)$ in Eq. (39) is determined from the solution of Eq. (40):

$$n_0(z) = \exp \left[- \int_z^{\infty} dz' \frac{1}{v(z')} R_0(z') \right]. \quad (41)$$

In the experiment all electrons with energies greater than E_A are collected. Thus, the normalized asymmetry measured in the experiment, $A^>(E_A)$, is given by Eq. (18) and is obtained from Eqs. (30) and (37) by

$$A^>(E_A) = \frac{a^>(E_A)}{N^>(E_A)}, \quad (42)$$

where

$$a^>(E_A) = \int_{E_A}^{\infty} dE'_A a(E'_A), \quad (43)$$

$$N^>(E_A) = \int_{E_A}^{\infty} dE'_A N(E'_A). \quad (44)$$

The quantity $a^>(E_A)$ is given by Eq. (30) with $\Delta I(E_A, z)$ and $I(E_A, z)$ replaced by $\Delta I^>(E_A, z)$ and $I^>(E_A, z)$, where

$$\Delta I^>(E_A, z) = \int_{E_A}^{\infty} dE'_A \Delta I(E'_A, z), \quad (45)$$

$$I^>(E_A, z) = \int_{E_A}^{\infty} dE'_A I(E'_A, z). \quad (46)$$

The quantity $N^>(E_A)$ is given by Eq. (37) with $I(E_A, z)$ replaced by $I^>(E_A, z)$.

It should be emphasized that the SPMDS measures the total production of Auger electrons rather than the rates of production measured in an experiment that detects currents. For example, assume that the rate r_{σ} is given by

$$r_{\sigma}(E_A, z) = g_{\sigma}(E_A) e^{-\alpha z} \quad (47)$$

for the production rate of Auger electrons where the decay of r_{σ} with z arises from the decay of the Ni wave functions in the vacuum region where they overlap the He atom. The asymmetry of the rates is

$$\frac{\dot{a}(E_A)}{\dot{N}(E_A)} = \frac{g_{\downarrow}(E_A) - g_{\uparrow}(E_A)}{g_{\downarrow}(E_A) + g_{\uparrow}(E_A)}. \quad (48)$$

From Eqs. (11) and (12)

$$N_{\sigma}(E_A) = \int dn_{\sigma} \frac{r_{\sigma}(E_A, z)}{R_{\sigma}(z)}, \quad (49)$$

where z is related to n_{σ} by Eq. (14). Use of Eq. (47) in Eq. (49) yields the total asymmetry

$$\frac{a(E_A)}{N(E_A)} = \frac{\bar{g}_{\downarrow}(E_A) - \bar{g}_{\uparrow}(E_A)}{\bar{g}_{\downarrow}(E_A) + \bar{g}_{\uparrow}(E_A)}, \quad (50)$$

where

$$\bar{g}_{\sigma}(E_A) = \frac{g_{\sigma}(E_A)}{\int_{-\infty}^{\infty} dE_A g_{\sigma}(E_A)}. \quad (51)$$

Unlike $\dot{a}(E_A)$, the asymmetry $a(E_A)$ satisfies the sum rule of Eq. (17), thus $a(E_A)$ must take both negative and positive values as a function of E_A . If the shape of the Auger distribution is spin independent so that $g_{\sigma}(E_A) = A_{\sigma} g(E_A)$, then $a(E_A) = 0$ while $\dot{a}(E_A)/\dot{N}(E_A) = (A_{\downarrow} - A_{\uparrow})/(A_{\downarrow} + A_{\uparrow})$. Clearly, asymmetry will in general be smaller than the asymmetry rate.

IV. AUGER PRODUCTION RATES

In this section we derive an approximate expression for $r_{\sigma}(E_A, z)$, the rate that Auger electrons are produced at energy E_A by an unfilled He spin σ 1s level located a distance z from the surface. The rate that spin \uparrow electrons are produced at E_A by a spin \downarrow hole in the He 1s level is

$$r_{\uparrow}^{(\downarrow)}(E_A, z) = \frac{2\pi}{\hbar} \sum_{k, n, k', n', k'', n''} |M_{1s \downarrow k' n' \uparrow}^{kn \downarrow k'' n''}|^2 \delta(E_{kn \downarrow} + E_{k' n' \uparrow} - E_{1s \downarrow} - E_{k'' n'' \uparrow}) \delta(E_A - E_{k'' n'' \uparrow}), \quad (52)$$

where

$$M_{\gamma\delta}^{\alpha\beta} = \int d^3 r_1 \int d^3 r_2 \psi_{\alpha}^*(1) \psi_{\gamma}(1) \frac{e^2}{r_{12}} \psi_{\beta}^*(2) \psi_{\delta}(2) \quad (53)$$

is the matrix element describing the Auger process and $e^2/r_{12}\epsilon$ is the screened Coulomb interaction. Equation (52) is simplified by the use of Kanès' random k approximation⁶⁷ in which momentum conservation is neglected. In Kanès treatment the matrix element is replaced by its average value. Here we allow it to depend on the energies of the states, $E_{kn\downarrow}$, $E_{k'n'\uparrow}$, E_{1s} , and $E_{k''n''\uparrow} = E_A$. The dependence of the matrix element M on $\epsilon = E_{kn\downarrow}$ and $\epsilon' = E_{k'n'\uparrow}$ will be written as $M(\epsilon, \epsilon')$ and the dependence of M on E_{1s} and E_A is assumed but not written explicitly. M is also dependent on the orbital character or the states; s - p -like or d -like. The Auger state with energy E_A must be s - p -like as it lies above the d band. It will become apparent that M is large only for those states, $E_{kn\downarrow}$, which have total momentum normal to the Ni surface. Within this approximation Eq. (52) becomes

$$r_{\downarrow}^{(\uparrow)}(E_A, z) = \frac{2\pi}{\hbar} \rho_s^>(E_A) \int d\epsilon \int d\epsilon' \sum_{l, l'} \rho_{l\downarrow}^<(\epsilon) \rho_{l'\uparrow}^<(\epsilon') |M^{ll'}(\epsilon, \epsilon')|^2 \delta(\epsilon + \epsilon' - E_A - E_{1s}), \quad (54)$$

where l is the orbital character of the state and

$$\rho_{l\sigma}^<(\epsilon) = \rho_{l\sigma}(\epsilon) f(\epsilon), \quad (55)$$

$$\rho_{l\sigma}^>(\epsilon) = \rho_{l\sigma}(\epsilon) [1 - f(\epsilon)], \quad (56)$$

where $\rho_{l\sigma}(\epsilon)$ is the density of states at energy ϵ for electrons of symmetry l and $f(\epsilon)$ is the Fermi factor. The matrix element $M^{ll'}(\epsilon, \epsilon')$ describes transitions from an electron in the state (ϵ, l) to the He $1s$ state and from an electron in the state (ϵ', l') to the Auger state (E_A, s) .

The matrix element $M^{ll'}(\epsilon, \epsilon')$ depends strongly on z because of the exponential decay of the metal wave function (ϵ, l) in the vacuum region. This is clear from Eq. (53), which shows that the matrix element is proportional to the overlap of the Ni wave function $\psi_{kn\downarrow}$ with the He⁺ ion. This overlap is maximized for metal states with total momentum normal to the metal surface and $\rho_{l\downarrow}(\epsilon)$ in Eq. (54) should be interpreted as the density of states with momentum normal to the surface.

The energy of the He $1s$ state, E_{1s} , in Eq. (54) is also a function of z due to the image potential of the Ni:

$$E_{1s} \equiv E_{1s}(z) = \frac{e^2}{4z} + E_{1s}^0, \quad (57)$$

where E_{1s}^0 is the energy of the He $1s$ state in the absence of Ni.

It is convenient to introduce the notation

$$C\{g(\epsilon, \epsilon')\} \equiv \frac{2\pi}{\hbar} \rho_s^>(E_A) \int \int_{\epsilon < \epsilon_F} d\epsilon \int_{\epsilon' < \epsilon_F} d\epsilon' g(\epsilon, \epsilon') \delta(\epsilon + \epsilon' - E_A - E_{1s}), \quad (58)$$

where ϵ_F is the Fermi energy. Equation (54) becomes

$$r_{\downarrow}^{(\uparrow)}(E_A, z) = C \left\{ \sum_{l, l'} \rho_{l\downarrow}^<(\epsilon) \rho_{l'\uparrow}^<(\epsilon') |M^{ll'}(\epsilon, \epsilon')|^2 \right\}. \quad (59)$$

The rate at which spin \downarrow electrons are produced by the He $1s \downarrow$ hole is

$$r_{\downarrow}^{(\downarrow)}(E_A, z) = C \left\{ \sum_{l, l'} \rho_{l\downarrow}^<(\epsilon) \rho_{l'\downarrow}^<(\epsilon') \frac{1}{2} |M^{ll'}(\epsilon, \epsilon') - M^{l'l}(\epsilon', \epsilon)|^2 \right\} \quad (60)$$

and the total rate is

$$r_{\sigma}(E_A, z) = r_{\sigma}^{(\uparrow)}(E_A, z) + r_{\sigma}^{(\downarrow)}(E_A, z). \quad (61)$$

Use of Eqs. (59)–(61) yields for $\Delta r = r_{\uparrow} - r_{\downarrow}$

$$\Delta r = C \left\{ \sum_{l, l'} [\rho_{l\uparrow}(\epsilon) \rho_{l'\uparrow}(\epsilon') - \rho_{l\downarrow}(\epsilon) \rho_{l'\downarrow}(\epsilon')] \frac{1}{2} |M^{ll'}(\epsilon, \epsilon') - M^{l'l}(\epsilon', \epsilon)|^2 \right. \\ \left. + [\rho_{l\uparrow}(\epsilon) \rho_{l'\downarrow}(\epsilon') - \rho_{l\downarrow}(\epsilon) \rho_{l'\uparrow}(\epsilon')] |M^{ll'}(\epsilon, \epsilon')|^2 \right\}. \quad (62)$$

The total rate $r_0 = (r_{\uparrow} + r_{\downarrow})$ is given by Eq. (62) with $\rho\rho - \rho\rho$ replaced by $\rho\rho + \rho\rho$. Equation (62) can be written as

$$\Delta r = C \left\{ \sum_{l, l'} m_l(\epsilon) n_{l'}(\epsilon') \left[|M^{ll'}(\epsilon, \epsilon')|^2 - \text{Re}\{M^{ll'}(\epsilon, \epsilon') [M^{l'l}(\epsilon', \epsilon)]^*\} \right] \right\}, \quad (63)$$

where

$$m_l(\epsilon) = \rho_{l\uparrow}(\epsilon) - \rho_{l\downarrow}(\epsilon), \quad (64)$$

$$n_l(\epsilon) = \rho_{l\uparrow}(\epsilon) + \rho_{l\downarrow}(\epsilon), \quad (65)$$

and

$$r = C \left\{ \sum_{l,l'} n_l(\epsilon) n_{l'}(\epsilon') |M^{ll'}(\epsilon, \epsilon')|^2 + \sum_{l,l'} \frac{1}{2} [n_l(\epsilon) n_{l'}(\epsilon') + m_l(\epsilon) m_{l'}(\epsilon')] \left[-\text{Re} \{ M^{ll'}(\epsilon, \epsilon') [M^{ll'}(\epsilon', \epsilon)]^* \} \right] \right\}. \quad (66)$$

In Ni the polarization is small so the magnetization can be neglected compared to the charge density and Eq. (66) becomes

$$r \approx C \left\{ \sum_{l,l'} n_l(\epsilon) n_{l'}(\epsilon') [|M^{ll'}(\epsilon, \epsilon')|^2 - \frac{1}{2} \text{Re} \{ M^{ll'}(\epsilon, \epsilon') [M^{ll'}(\epsilon', \epsilon)]^* \}] \right\}. \quad (67)$$

Using the fact that the He 1s wave function is very compact the matrix element in Eq. (53) can be approximated by

$$M_{ls\delta}^{\alpha\beta} \approx \psi_{\alpha}(\mathbf{R}_{\text{He}}) \Phi_{\delta}^{\beta} \quad (68)$$

where \mathbf{R}_{He} is the position of the He atom and

$$\Phi_{\delta}^{\beta} = \left[\int d^3r \psi_{1s}(\mathbf{r}) \right] \int d^3r \frac{e^2}{|\mathbf{R}_{\text{He}} - \mathbf{r}| \epsilon} \psi_{\beta}^*(\mathbf{r}) \psi_{\delta}(\mathbf{r}). \quad (69)$$

The Ni wave function at the He position, $\psi_{kn}(\mathbf{R}_{\text{He}})$, will be largest for values of total momentum normal to the surface. Thus, in Eq. (54), $M^{ll'}(\epsilon, \epsilon')$ can be written

$$M^{ll'}(\epsilon, \epsilon') = \psi_{l,\epsilon}(\mathbf{R}_{\text{He}}) \Phi_{l',\epsilon'}^*, \quad (70)$$

where $\psi_{l,\epsilon}$ is a metal wave function with energy ϵ and total momentum normal to the surface. If the interference terms in Eqs. (63) and (67) are neglected, use of Eq. (70) in those equations gives

$$\Delta r = C \left\{ \sum_{l,l'} m_l(\epsilon, R_{\text{He}}) n_{l'}(\epsilon') |\Phi_{l',\epsilon'}|^2 \right\}, \quad (71)$$

$$r = C \left\{ \sum_{l,l'} n_l(\epsilon, R_{\text{He}}) n_{l'}(\epsilon') |\Phi_{l',\epsilon'}|^2 \right\}, \quad (72)$$

where

$$m_l(\epsilon, R_{\text{He}}) = m_l(\epsilon) |\psi_{l,\epsilon}(\mathbf{R}_{\text{He}})|^2, \quad (73)$$

$$n_l(\epsilon, R_{\text{He}}) = n_l(\epsilon) |\psi_{l,\epsilon}(\mathbf{R}_{\text{He}})|^2. \quad (74)$$

It is understood that in the integration over ϵ in Eq. (71) [implied by $C\{\}$] only those states are summed over which have momentum normal to the surface.

The quantities $m_l(\epsilon, R_{\text{He}})$ and $n_l(\epsilon, R_{\text{He}})$ represent the magnetization density and number density of Ni electrons at the He atom for electrons of symmetry l . From band calculations⁶⁸ the d magnetization in bulk Ni is $m_d \sim 0.6\mu_B$ per atom for the d electrons and $m_s \sim -0.02\mu_B$ per atom for the s - p electrons. However, at a distance of 1.2 Å into the vacuum $m_d \sim 0.0\mu_B$ and $m_s \sim -0.005\mu_B$. The number of electrons at that distance is $n_s \sim 0.14$ so the s electron polarization is $p_s \sim -3.5\%$.

In order for Eq. (28) to agree with the measured sign of the asymmetry, Δr must be negative. Thus the dominant contribution to Δr in Eq. (71) must correspond to $m_l < 0$ which is consistent with $m_s \sim -0.005\mu_B$ per atom and $m_d \sim 0$. Following this discussion it is assumed that the Ni d magnetization and charge density at the He⁺ ion

can be neglected, thus Eq. (71) gives

$$\Delta r \approx C \left\{ m_s(\epsilon, R_{\text{He}}) \sum_l n_l(\epsilon') |\Phi_{l',\epsilon'}|^2 \right\}, \quad (75)$$

$$r \approx C \left\{ n_s(\epsilon, R_{\text{He}}) \sum_l n_l(\epsilon') |\Phi_{l',\epsilon'}|^2 \right\}. \quad (76)$$

An expression for the normalized asymmetry at the highest observable Auger energy E_A^0 , defined in Eq. (8), is easily obtained. The largest Auger energy is obtained when the Auger transition involves two metal electrons with energies equal to the Fermi energy. Furthermore, as is apparent from Eq. (57), the He 1s level, $E_{1s}(z)$, lies lowest when the He⁺ ion is far from the Ni surface. If we observe Auger transitions with energies E_A or larger, then it follows from Eq. (57) that z must be greater than z_{\min} , where $z_{\min} = (e^2/4)(E_A^0 - E_A)^{-1}$ and the integration over z in Eqs. (30) and (37) is restricted to $z > z_{\min}$. As $E_A \rightarrow E_A^0$, Eqs. (28) and (29) yield

$$A^>(E_A^0) = \frac{a^>(E_A^0)}{N^>(E_A^0)} = \frac{-\Delta r(E_A^0, z \rightarrow \infty)}{r_0(E_A^0, z \rightarrow \infty)} \quad (77)$$

and Eq. (77) gives the integrated normalized asymmetry as

$$A^>(E_A^0) = -p_s(\epsilon_F, R_{\text{He}}), \text{ as } R_{\text{He}} \rightarrow \infty, \quad (78)$$

where $p_s(\epsilon_F, R_{\text{He}})$ is the polarization at energy ϵ_F of the metal s - p electrons at the He⁺ ion. If the s polarization is constant outside the surface, then $A^>(E_A^0) = -p_s(\epsilon_F, z_v)$, where z_v is the distance from the surface at which the d electron density becomes negligible, $z_v \sim 1-2$ Å.

If this were the same as the average polarization just outside the metal it would imply $A^>(E_A^0) \approx 3.5\%$, however the s - p polarization at the Fermi energy is probably larger than the average polarization. The s - p polarization is due to s - d hybridization with the spin-polarized d bands and would be zero if the d -band polarization was zero. Assuming $|p_s(\epsilon)| \propto |p_d(\epsilon)|$ implies that $p_s(\epsilon)$ increases linearly with energy, thus $p_s(\epsilon_F)$ is on the order of four times the average polarization, p_s , in the s - p band, which means that $A^>(E_A^0) \approx 14\%$, in reasonable agreement with the experimental results.

In order to carry out numerical calculations it is necessary to model $\Delta r(E_A, z)$ and $r(E_A, z)$ given by Eqs. (75) and (76). The quantities $m_s(\epsilon, R_{\text{He}})$ and $n_s(\epsilon, R_{\text{He}})$ depend on $|\psi_{s,\epsilon}(\mathbf{R}_{\text{He}})|^2$, the s component of the Ni wave

function at the He ion. The simplest approximation for $\psi_{s,\epsilon}(z)$ is

$$\psi_{s,\epsilon}(z) \propto e^{-\gamma z}, \quad (79)$$

where

$$\gamma = \left[\frac{2m}{\hbar^2} (\varphi - \epsilon_1) \right]^{1/2}, \quad (80)$$

where φ is the Ni work function and ϵ_1 is the "normal component" of the electron energy. In a free electron metal $\epsilon_1 = \epsilon - (\hbar^2/2m)k_{\parallel}^2$, where k_{\parallel} is the momentum parallel to the surface. The corresponding d component can be estimated from⁶⁹

$$\psi_{d,\epsilon}(z) = e^{-\gamma(z+a/2)}, \quad (81)$$

where $a/2$ is the distance of the Ni atoms from the jellium edge and $a = 3.52 \text{ \AA}$ is the Ni lattice constant. Consequently $\psi_d/\psi_s \approx 0.15$, which is consistent with the neglect of the d magnetization and number density at the He ion.

It will be seen that a more accurate approximation for $\psi_{s,\epsilon}(z)$ will be required to obtain agreement with the experimental results.

Equation (79) holds if the potential in the region between the Ni surface and the He⁺ ion is a rectangular barrier. However, the potential of an electron in the vacuum region should include the metal image potential as well as the potential of the He⁺ ion and its image

$$V(z_e; z) = -\frac{e^2}{4z_e} - \frac{e^2}{|z - z_e|} + \frac{e^2}{|z + z_e|}, \quad (82)$$

where z_e is the z component electron coordinate and z is

the distance of the He⁺ ion from the Ni surface. The WKB approximation can be used to estimate the decay of the Ni wave function for the state with s - p symmetry and energy ϵ ,

$$\psi_{s,\epsilon}(z) = \exp \left[- \int dz_e \kappa(z_e; z, \epsilon) \right], \quad (83)$$

where

$$\kappa(z_e; z; \epsilon) = \left[\frac{2m}{\hbar^2} [\varphi - \epsilon + V(z_e, z)] \right]^{1/2} \quad (84)$$

The integration in Eq. (83) is from the left turning point to the right turning point and it has been assumed that we are considering a state with total momentum normal to the metal surface in Eq. (84).

The terms due to the He⁺ ion on the right-hand side of Eq. (82) are often not included in problems involving ion-surface interactions, however they make a major change in the potential barrier. The most probable distance of the He⁺ atom from the surface for Auger production, z_A , is given by the maximum of $R_0(z)n_0(z)/v(z)$. For the rectangular potential barrier, Eq. (79) leads to $z_A \approx 1-2 \text{ \AA}$ while Eqs. (82) and (83), which include image and He⁺ potentials, give $z_A \approx 4-5 \text{ \AA}$ as will be discussed in the next section.

$\Phi_l(\epsilon)$ in Eq. (70) will be a slowly varying function of z and ϵ and is taken to be constant, Φ_l . Defining

$$n(\epsilon) \equiv \frac{\sum_l n_l(\epsilon) |\Phi_l|^2}{\sum_l |\Phi_l|^2} \quad (85)$$

Equation (71) for Δr and r_0 can be written explicitly as

$$\Delta r(E_A, z) = \gamma \int_{-\infty}^{\infty} d\epsilon \int_{-\infty}^{\infty} d\epsilon' m_s(\epsilon) |\psi_{s,\epsilon}(z)|^2 n(\epsilon') \delta(E_A + E_{1s}(z) - \epsilon - \epsilon'), \quad (86)$$

$$r_0(E_A, z) = \gamma \int_{-\infty}^{\infty} d\epsilon \int_{-\infty}^{\infty} d\epsilon' n_s(\epsilon) |\psi_{s,\epsilon}(z)|^2 n(\epsilon') \delta(E_A + E_{1s}(z) - \epsilon - \epsilon'), \quad (87)$$

where

$$\gamma = \frac{2\pi}{\hbar} \rho_s^>(E_A) \sum_l |\Phi_l|^2, \quad (88)$$

where $m_s(\epsilon)$, $n_s(\epsilon)$ are given by Eqs. (64) and (65), $E_{1s}(z)$ is given by Eq. (57), and γ is assumed constant.

V. RESULTS

The total asymmetry is obtained from Eqs. (28), (29), (43), and (44) as

$$A^>(E_A) = \frac{a^>(E_A)}{N^>(E_A)},$$

where

$$a^>(E_A) = -2 \int_0^{\infty} dz \frac{1}{v(z)} n_0(z) \left[\Delta r^>(E_A, z) - r_0^>(E_A, z) \int_z^{\infty} dz' \frac{1}{v(z')} \Delta R(z') \right], \quad (89)$$

where

$$n_0(z) = \exp \left[- \int_z^{\infty} dz' R_0(z')/v(z') \right],$$

$$R_0(z) = r_0^>(-\infty, z), \quad (90)$$

$$\Delta R(z) = \Delta r^>(-\infty, z), \quad (91)$$

and

$$r_0^>(E_A, z) = \int_{E_A}^{\infty} dE'_A r_0(E'_A, z), \quad (92)$$

$$\Delta r^>(E_A, z) = \int_{E_A}^{\infty} dE'_A \Delta r(E'_A, z), \quad (93)$$

and

$$N^>(E_A) = 2 \int_0^\infty dz \frac{1}{v(z)} n_0(z) r_0^>(E_A, z). \quad (94)$$

Thus, $A^>(E_A)$ can be calculated once $r_0(E_A, z)$ and $\Delta r(E_A, z)$ are known. These two quantities are given by Eqs. (86) and (87) and are specified by choosing a model for $m_s(\epsilon)$, $n_s(\epsilon)$, and $n(\epsilon)$. The asymmetry is not sensitive to the detailed energy dependence of these quantities because they enter Δr and r through a convolution. The magnetization $m_s(\epsilon)$ is due to hybridization of the s bands with the d bands and would be zero if the d -band magnetization were zero. We assume that $m_s(\epsilon) \propto -m_d(\epsilon)$, where $m_d(\epsilon)$ is the magnetization density of the d states which is roughly a linear function of ϵ . Thus

$$m_s(\epsilon) = -a(\epsilon + W_d), \quad \text{for } -W_d < \epsilon, \quad (95)$$

where W_d is the width of the d band and a will be specified. The density of s electrons is taken to be constant:

$$n_s(\epsilon) = b, \quad \text{for } -W_s < \epsilon, \quad (96)$$

where W_s is the depth of the s band below the Fermi level. We take $W_d = 5$ eV, $W_s = 10$ eV, and b will be specified. Finally $n(\epsilon)$ is the density of states associated with excitations of Auger electrons from Ni and it is taken to be a linear combination of s -like and d -like density of states

$$n(\epsilon) = c[(1-\lambda)\Theta(\epsilon + W_s) + \lambda(\epsilon + W_d)\Theta(\epsilon + W_d)], \quad (97)$$

where the unit-step function $\Theta(x) = 1$ if $x > 0$ and $\Theta(x) = 0$ if $x < 0$, and λ determines the relative amount of s and d character of the states from which the Ni Auger electrons originate. From Eqs. (86) and (87) it is clear that for a given λ there are two free parameters, γac and γbc . Rather than specifying these we choose as one parameter

$$L = -\ln n_0(0), \quad (98)$$

where $n_0(0)$ is the fraction of He ions that reach the Ni surface without neutralizing. From Eq. (26)

$$L = \int_0^\infty dz \frac{R_0(z)}{v(z)} \quad (99)$$

so that specifying L is equivalent to specifying γbc .

A second parameter is determined by requiring that the calculated value of $A^>(E_A)$ (for a specific choice of λ and L) agrees with the experimental value of $A^>(E_A)$ for a particular E_A . This adjusts the scale of the calculated asymmetry.

Aside from $m_s(\epsilon)$, $n_s(\epsilon)$, and $n(\epsilon)$ the quantities $r_0(E_A, z)$ and $\Delta r(E_A, z)$ involve $|\psi_{s,\epsilon}(z)|^2$ as is seen from Eqs. (86) and (87). This quantity represents the density of metal electrons at the position of the He ion and it is given by

$$|\psi_{s,\epsilon}(z)|^2 = e^{-\gamma(z,\epsilon)}, \quad (100)$$

where

$$\gamma(z,\epsilon) = 2 \int dz_e \kappa(z_e; z, \epsilon) \quad (101)$$

and where κ is given by Eq. (84). In Eq. (100), z is the metal-ion distance and ϵ is the energy of the metal electron. The quantity $\gamma(z,\epsilon)$ is plotted as a function of z in Fig. 3 for various values of ϵ . It is clear from the figure that γ may be approximated by

$$\gamma(z,\epsilon) \approx a(\epsilon)[z - z_0(\epsilon)], \quad (102)$$

where $z_0(\epsilon)$ has a strong dependence on ϵ and $a(\epsilon)$ has a weak dependence. For a rectangular barrier model $a \sim 2(2m\phi/\hbar^2)^{1/2} \approx 2.3 \text{ \AA}^{-1}$, whereas $a(\epsilon_F) \approx 1.4 \text{ \AA}^{-1}$ because of the lower height of the more realistic barrier. Unlike the rectangular barrier, this barrier goes to zero for distances less than $z_0(\epsilon)$ for electrons with energy ϵ . For electrons at the Fermi energy $z_0(\epsilon_F) \approx 4.1 \text{ \AA}$ while $z_0(\epsilon_F - 3 \text{ eV}) \approx 2.5 \text{ \AA}$.

The total asymmetry is now calculated only allowing for transitions from states of s symmetry, $\lambda = 0$ in Eq. (97). For every value of the parameter L of Eq. (98) the theoretical curve is normalized in such a way that it falls within the experimental error bars for the point $E_A = 9$ eV. As shown in Fig. 4 it is found that for values of L such that $31 < L < 35$ the theoretical $A^>(E_A)$ is in agreement with the experiment³⁶ for all measured values of E_A . For a value of $L = 32$ the quantities $n_0(z)$ [given by Eq. (26)], $R_0(z)/v(z)$ [given by Eq. (90)], and $n_0(z)[R_0(z)/v(z)]$ are plotted versus z in Fig. 5. The product $n_0 R_0/v$ represents the average number of He ions that are ionized per unit distance and it has a pronounced peak in agreement with the much simpler theory, Eqs. (2)–(7), but the peak is at 4.5 \AA rather than considerably closer to the surface as predicted by Eqs. (2)–(7). Thus ionization takes place $\sim 4.5 \text{ \AA}$ from the surface, a considerably larger distance than previous estimates.^{51–55}

This difference is due in large part to the term $z_0(\epsilon)$ in Eq. (102), in other words to the very different shape of the real potential, Eq. (84), from a rectangular potential.

A rough estimate of the quantity R_0 that appears in

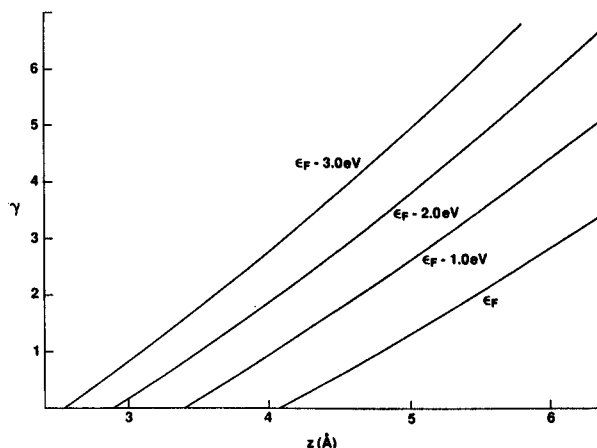


FIG. 3. Dependence of the exponential decay factor, $\gamma(z,\epsilon)$, of Eq. (100) on the Ni-He⁺ distance and on the electron energy.

the simple expression $R = R_0 e^{-a(z-z_0)}$ can be obtained by estimating R_0 from

$$L = \int_0^\infty dz \frac{R(z)}{v(z)} \approx \int_{z_0}^\infty dz \frac{R_0}{v(z)} e^{-a(z-z_0)}, \quad (103)$$

where use has been made of Eq. (102) and the ϵ dependence of a and z_0 have been neglected. For $z_0 = 4.5 \text{ \AA}$ and $a = 1.6 \text{ \AA}^{-1}$ as determined from Figs. 3 and 5 we find $R_0 \approx 10^{14} \text{ s}^{-1} \text{ L}$ or $R_0 \approx 3 \times 10^{15} \text{ s}^{-1}$, in reasonable agreement with other estimates of R_0 .

As shown by Eq. (78), the asymmetry evaluated at the maximum value of E_A yields the polarization of the Ni far from the surface at an energy equal to the Fermi energy. This asymmetry cannot be obtained directly from the experimental values because of the enormous experimental uncertainty in $A^>(E_A)$ for large E_A . However, determining parameters such that the theory agrees with experiment for all measured values of E_A then allows an extrapolation to E_A^0 via the theoretical calculations for $A^>(E_A)$ and hence a determination of the polarization,

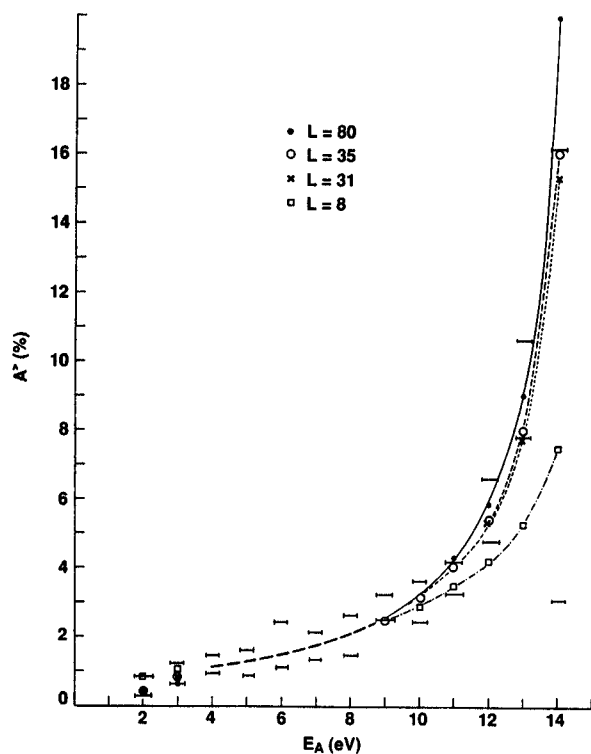


FIG. 4. Comparison of theory and experiment for the integrated asymmetry measured in Ref. 36. Several values of the parameter L [defined in Eqs. (98) and (99)] are chosen and the theoretical curves are scaled so they agree with experiment at $E_A = 9 \text{ eV}$. The magnetization density is given by Eq. (95) and $\lambda = 0$ in Eq. (97). The experimental error bars from Fig. 1 are indicated. In the region $4 \leq E_A \leq 9$ the curves for $L = 8, 31, 35$, and 80 are essentially identical. The theoretical results for $A^>$ corresponding to $L = 31$ and $L = 35$ fall within all the experimental error bars.

Eq. (78). For $31 < L < 35$ this gives $22\% < |p_s(\epsilon_F, z \rightarrow \infty)| < 24\%$. It has been assumed that the polarization does not change with distance from the surface for distances larger than several angstroms. This extrapolated value of p_s is larger than the estimate from band theory.

A magnetization density given by Eq. (95) implies the polarization at ϵ_F to be four times the polarization determined by band theory⁶⁸ (which is an average over the entire band) at a distance 1.2 \AA into the vacuum; $p_s(\epsilon_F, z = 1.2 \text{ \AA}) = 4p_s = -14\%$, which should be compared to the estimate for p_s in the previous paragraph. However, the value $p_s \approx -3.5\%$ is at the limits of the accuracy of the band calculation since it corresponds to a magnetization of only $\approx 0.005 \mu_B$ per atom. Furthermore, it is not clear that 1.2 \AA is sufficiently far from the surface for p_s to have reached its asymptotic value.

There are a number of changes in the model that can reasonably be made. The parameter λ in Eq. (97) can be varied to allow for some d character in the states from which the Auger electrons are produced. It is still possible to obtain fits to the experimental results for $A^>(E_A)$ for values up to $\lambda \approx 0.6$. The magnetization density $m_s(\epsilon)$ in Eq. (95) can be taken to be quadratic in energy and a fit to the experimental data can be obtained for $24 < L < 32$ for $\lambda = 0$. Similarly the barrier shape given

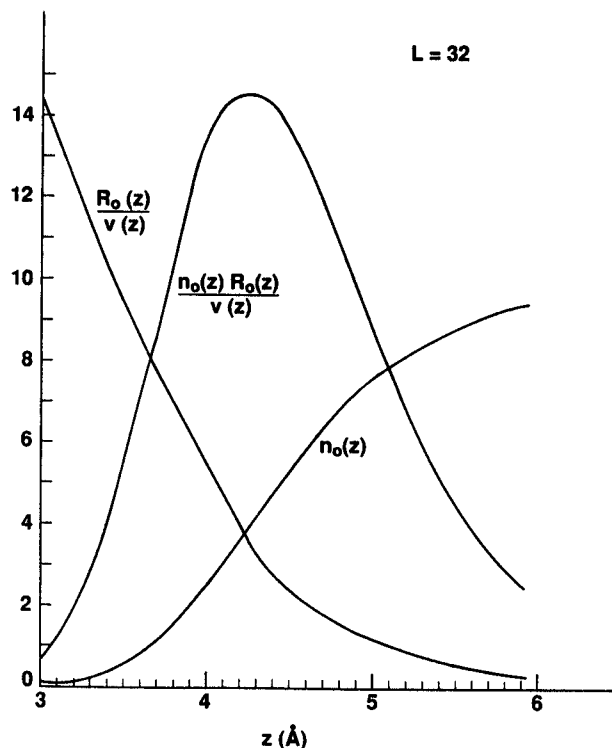


FIG. 5. The number of He^+ ions $n_0(z)$, the neutralization rate per unit distance $R_0(z)/v(z)$, and the filling probability $P_0(z) = n_0(z)R_0(z)/v(z)$, are shown for the case $L = 32$ of Fig. 4. The value of z for which $P_0(z)$ is a maximum is roughly the most probable distance for neutralization. The actual most probable distance depends on electron energy.

by Eq. (82) can be somewhat altered to compensate for the assumption of one dimensionality. A more realistic three-dimensional potential might result in a preexponential factor in Eq. (82) that varies with distance. It is found that a factor $1/(1+bz^n)^{1/2}$ for $n=1,2,3$ and $0.5 < b < 4$ will allow a fit to the experiment by choosing a suitable value of L . Other values of b, n as well as other functional forms would probably work as well. However, if $m_s(\epsilon)$ is assumed constant, then a fit cannot be obtained. Also, the assumed barrier potential, Eq. (82), cannot be changed in a fundamental way if a fit is to be made. The energy dependence of $\psi_{s,\epsilon}(z)$ is required if theory is to agree with experiment. Similarly, the approximation to $\psi_{s,\epsilon}(z)$ obtained from Eq. (102) for z_0 independent of ϵ will not yield a fit. In particular, the usual rectangular barrier model where $z_0(\epsilon)=0$ will not reproduce the experimental results. In short, the agreement between theory and experiment only obtains for barrier potentials similar in shape to that described by Eq. (82).

VI. SUMMARY

The qualitative explanation of the experimental asymmetry is as follows. The number of electrons of spin σ with energies greater than E_A produced by incoming He^+ ions with $1s$ spin σ holes is from Eqs. (11) and (19):

$$N_\sigma^>(E_A) = \int_0^\infty dz P_\sigma(z) I_\sigma^>(E_A, z), \quad (104)$$

where

$$P_\sigma(z) = \frac{R_\sigma(z) n_\sigma(z)}{v(z)} \quad (105)$$

and

$$I_\sigma^>(E_A, z) = \frac{r_\sigma^>(E_A, z)}{r_\sigma^>(-\infty, z)} \quad (106)$$

and

$$r_\sigma^>(E_A, z) = \int_{E_A}^\infty dE'_A r_\sigma(E'_A, z), \quad (107)$$

where use has been made of the relation $R_\sigma(z) = r_\sigma^>(-\infty, z)$.

In Eq. (104) the quantity $P_\sigma(z)$ is the probability that a He^+ ion with a $1s$ spin σ hole is neutralized at a distance z from the surface. In Eq. (105), $R_\sigma(z)/v(z)$ is the probability per unit distance per ion of neutralization and $n_\sigma(z)$ is the number of ions. The quantity $I_\sigma^>(E_A, z)$ is the normalized integrated Auger spectrum. It represents the fraction of Auger electrons produced with energies greater than E_A by the He^+ ions. The rate at which the He^+ ions fill the $1s$ spin σ holes and produce Auger electrons with energies greater than E_A is $r_\sigma^>(E_A, z)$ which is obtained by integrating the rate $r_\sigma(E'_A, z)$, over all energies greater than E_A , Eq. (107).

The quantity $P_\sigma(z)$ peaks at a distance z_σ from the surface. Because the He ions with spin \downarrow holes fill at a faster rate than those with spin \uparrow , it follows that $z_\downarrow > z_\uparrow$. This difference in filling rates is due to the excess of spin \downarrow s metal electrons over spin \uparrow s electrons outside the Ni surface. The Auger spectrum $I_\sigma^>(E_A, z)$ is a function of dis-

tance from the surface primarily because of the image potential which shifts the spectrum. As the He ion moves closer to the surface the position of the $1s$ level moves to higher energy due to the image potential of the Ni. Thus the entire Auger spectrum is shifted to lower energies as z decreases. The normalized Auger spectrum is shown schematically in Fig. 6 as a function of z assuming it to be independent of σ . Also sketched are $P_\uparrow(z)$ and $P_\downarrow(z)$. For a given value of E_A and for a given z all electrons with energies greater than E_A in the normalized Auger spectrum are collected. The number of spin σ electrons collected is obtained by multiplying this quantity by $P_\sigma(z)$ and integrating over z . For a given E_A there is a minimum value of z which contributes to the integration in Eq. (104); this occurs when the maximum Auger energy falls below E_A as indicated in Fig. 6. For small E_A this happens quite near the surface and the integration over z includes all the area under $P_\uparrow(z)$ and $P_\downarrow(z)$ so that $N_\uparrow^>(E_A), N_\downarrow^>(E_A) \approx 1$ and $A^>(E_A) \approx 0$. For larger values of E_A the integration over z will include more of the area of $P_\downarrow(z)$ than $P_\uparrow(z)$ with the result $A^>(E_A) > 0$. The precise shape of $A^>(E_A)$ depends on the shapes of the peaks in $P_\sigma(z)$ and their positions. The further the peaks in P_σ from the surface the greater the slope of $A^>(E_A)$.

We have found the following. (1) The integrated asymmetry measures the Ni magnetization outside the surface (at the He ion). Assuming that the s electron polarization is constant in the vacuum it is possible to extract the Ni polarization at the Fermi energy far from the surface (> 2 Å) from the experimental results. This is estimated to be

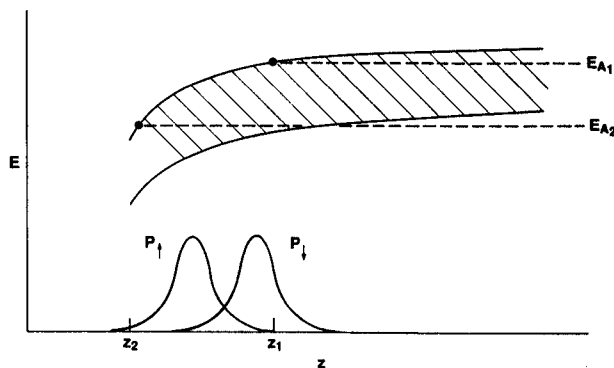


FIG. 6. Explanation for the dependence of the asymmetry, $A^>$, on E_A . For a given z , the shaded region indicates the range of energies to which Ni Auger electrons are excited due to He^+ neutralization. The z dependence is due to the influence of the image potential on the He^+ $1s$ level. The probabilities for neutralization of spin \uparrow and spin \downarrow He $1s$ holes, P_\uparrow and P_\downarrow , are shown schematically. For large E_A , $E_A = E_{A1}$, neutralization and Auger production of electrons with energies $E_A \geq E_{A1}$ can take place only for $z > z_1$, where $P_\uparrow(z) \approx 0$. Thus, primarily He^+ $1s$ \downarrow holes are filled and $A^>(E_{A1})$ is larger. For small E_A , $E_A = E_{A2}$, both P_\uparrow, P_\downarrow are large in the region $z > z_2$ and He^+ $1s$ holes with both spins are filled so that $A^>$ is small.

$\approx -20\%$. (2) The experimental results³⁶ are reproduced by the theory with the use of two parameters, one that specifies the magnitude of the ionization rate and one that adjusts the scale of the calculated asymmetry. (3) This fit is only possible with a realistic, energy-dependent expression for the tunneling barrier seen by a metal electron and produced by the He ion. The ionization takes place at an average distance of ~ 4.5 Å from the surface for a metal electron at the Fermi energy and at smaller distances for lower energy electrons. (4) A fit to the experimental results can be obtained for various reasonable models of the energy dependence of the Ni magnetization and the Ni Auger spectrum without any substantial

changes in the previously quoted numbers. However, a fit cannot be obtained for an energy-independent Ni magnetization density, nor for the case where the dominant contribution to the Auger spectrum is from *d* states rather than *s-p* states.

ACKNOWLEDGMENTS

We would like to thank Dr. K. Walters and Dr. C. Monreal for a number of very useful discussions throughout the course of this work.

- ¹D. T. Pierce and R. J. Celotta, *Adv. Electron. Electron Phys.* **56**, 219 (1982).
- ²F. B. Dunning, C. Rau, and G. K. Walters, *Comments Solid State Phys.* **12**, 17 (1986).
- ³J. Kirschner, D. Rebenstorff, and H. Ibach, *Phys. Rev. Lett.* **53**, 698 (1984).
- ⁴J. Glazer and E. Tosatti, *Solid State Commun.* **52**, 905 (1984).
- ⁵H. Hopster, R. Raue, and R. Clauberg, *Phys. Rev. Lett.* **53**, 695 (1984).
- ⁶J. Unguris, D. T. Pierce, A. Galejs, and R. J. Celotta, *Phys. Rev. Lett.* **49**, 72 (1982).
- ⁷E. Kisker, W. Gudat, and K. Schröder, *Solid State Commun.* **44**, 591 (1982).
- ⁸H. Hopster, R. Raue, E. Kisker, G. Güntherodt, and M. Campagna, *Phys. Rev. Lett.* **50**, 70 (1983).
- ⁹M. Landolt and D. Mauri, *Phys. Rev. Lett.* **49**, 1783 (1982).
- ¹⁰J. Glazer, Ph.D. thesis, University of Trieste, 1984.
- ¹¹D. R. Penn, S. P. Apell, and S. M. Girvin, *Phys. Rev. Lett.* **55**, 518 (1985); *Phys. Rev. B* **32**, 7753 (1985).
- ¹²J. F. Cooke, J. A. Blackman, and T. Morgan, *Phys. Rev. Lett.* **54**, 718 (1985).
- ¹³H. C. Siegmans, *Physica (Amsterdam)* **127B**, 131 (1984).
- ¹⁴J. Kirschner, *Phys. Rev. Lett.* **55**, 973 (1985).
- ¹⁵J. Unguris, A. Seiler, R. J. Celotta, D. T. Pierce, P. D. Johnson, and N. V. Smith, *Phys. Rev. Lett.* **49**, 1047 (1982).
- ¹⁶H. Scheidt, M. Glübl, V. Dose, and J. Kirschner, *Phys. Rev. Lett.* **51**, 1688 (1983).
- ¹⁷G. Busch, M. Campagna, and H. C. Siegmans, *Phys. Rev. B* **4**, 746 (1971).
- ¹⁸S. F. Alvarado, *Z. Phys. B* **33**, 51 (1979).
- ¹⁹E. Kisker, *J. Phys. Chem.* **87**, 3597 (1983).
- ²⁰D. G. Dempsey and L. Kleinman, *Phys. Rev. Lett.* **39**, 1297 (1977).
- ²¹L. Kleinman, *Comments Solid State Phys.* **10**, 29 (1981).
- ²²D. E. Eastman, J. F. Janak, A. R. Williams, R. V. Coleman, and G. Wendin, *J. Appl. Phys.* **50**, 7423 (1979).
- ²³R. Allenspach and M. Landolt, *Surf. Sci.* **171**, L479 (1986).
- ²⁴M. Landolt, R. Allenspach, and D. Mauri, *J. Appl. Phys.* **57**, 3626 (1985).
- ²⁵K. Schröder, E. Kisker, and A. Bringer, *Solid State Commun.* **55**, 377 (1985).
- ²⁶D. Paraskevopoulos, R. Meserve, and P. M. Tedrow, *Phys. Rev. B* **16**, 4907 (1977).
- ²⁷D. Nagy, *Surf. Sci.* **90**, 102 (1979).
- ²⁸R. Meserve and P. M. Tedrow, *Solid State Commun.* **11**, 333 (1972).
- ²⁹J. S. Moodera and R. Meserve, *Phys. Rev. B* **29**, 2943 (1984).
- ³⁰R. J. Celotta, D. T. Pierce, G.-C. Wang, S. D. Bader, and G. P. Felcher, *Phys. Rev. Lett.* **43**, 728 (1979).
- ³¹S. F. Alvarado, M. Campagna, and H. Hopster, *Phys. Rev. Lett.* **48**, 51 (1982).
- ³²C. Rau and R. Sizmann, *Phys. Lett. A* **43**, 317 (1973).
- ³³C. Rau, *J. Magn. Magn. Mater.* **30**, 141 (1982).
- ³⁴C. Rau, *Appl. Surf. Sci.* **13**, 310 (1982).
- ³⁵D. W. Gidley, A. R. Köymen, and T. W. Capehart, *Phys. Rev. Lett.* **49**, 1779 (1982).
- ³⁶M. Onellion, M. W. Hart, F. B. Dunning, and G. K. Walters, *Phys. Rev. Lett.* **52**, 380 (1984).
- ³⁷M. W. Hart, M. S. Hammond, F. B. Dunning, and G. K. Walters, *Phys. Rev. B* **39**, 5488 (1989).
- ³⁸R. N. Varney, *Phys. Rev.* **157**, 116 (1967); **175**, 98 (1968).
- ³⁹D. A. MacLennan *et al.*, *J. Chem. Phys.* **50**, 1772 (1969); **50**, 1779 (1969).
- ⁴⁰F. B. Dunning *et al.*, *J. Phys. B* **4**, 1683 (1971); **4**, 1696 (1971); **4**, 1175 (1972).
- ⁴¹T. Shibata, T. Hirooka, and K. Kuchitau, *Chem. Phys. Lett.* **30**, 241 (1975).
- ⁴²C. Boizeau, V. Dose, and J. Roussel, *Surf. Sci.* **61**, 412 (1976).
- ⁴³P. D. Johnson and T. A. Delchar, *Surf. Sci.* **77**, 400 (1978).
- ⁴⁴S.-W. Wang and G. Ertl, *Surf. Sci.* **93**, L75 (1980).
- ⁴⁵H. Conrad, G. Ertl, J. Küppers, and W. Sesselmann, *Surf. Sci.* **121**, 161 (1982).
- ⁴⁶W. Sesselmann, B. Woratschek, G. Ertl, J. Küppers, and H. Haberland, *Surf. Sci.* **146**, 17 (1984).
- ⁴⁷E. Hood, F. Bozso, and H. Metiu, *Surf. Sci.* **161**, 491 (1985).
- ⁴⁸F. von Trentini and G. Doyen, *Surf. Sci.* **162**, 971 (1985).
- ⁴⁹J. Lee, C. Hanrahan, J. Arias, F. Bozso, R. M. Martin, and H. Metiu, *Phys. Rev. Lett.* **54**, 1440 (1985).
- ⁵⁰B. Woratschek, W. Sesselmann, J. Küppers, G. Ertl, and H. Haberland, *Phys. Rev. Lett.* **55**, 611 (1985).
- ⁵¹H. D. Hagstrum, *Phys. Rev.* **96**, 336 (1954).
- ⁵²H. D. Hagstrum, *Phys. Rev.* **150**, 495 (1966).
- ⁵³H. D. Hagstrum and G. E. Becker, *Phys. Rev.* **159**, 572 (1967).
- ⁵⁴H. D. Hagstrum, *Phys. Rev.* **122**, 83 (1961).
- ⁵⁵J. A. Appelbaum and D. R. Hamann, *Phys. Rev. B* **12**, 5590 (1975).
- ⁵⁶J. C. Tully, *Phys. Rev. B* **16**, 4324 (1977).
- ⁵⁷U. von Gemmingen and R. Sizmann, *Surf. Sci.* **114**, 445 (1982).
- ⁵⁸A. Cobas and W. E. Lamb, *Phys. Rev.* **65**, 327 (1944).
- ⁵⁹M. L. E. Oliphant, *Proc. R. Soc. London, Ser. A* **124**, 228 (1929).
- ⁶⁰H. S. W. Massey, *Proc. Cambridge Philos. Soc.* **26**, 386 (1930); **27**, 460 (1931).
- ⁶¹R. K. Janev and N. N. Nedeljković, *J. Phys. B* **7**, 1506 (1974); **14**, 2995 (1981); **18**, 915 (1985).

- ⁶²V. Heine, Phys. Rev. **151**, 561 (1966).
⁶³W. Eib and S. F. Alvarado, Phys. Rev. Lett. **37**, 444 (1976).
⁶⁴V. L. Moruzzi, J. F. Janak, and A. R. Williams, *Calculated Properties of Metals* (Pergamon, New York, 1978).
⁶⁵D. G. Dempsey, W. R. Grise, and L. Kleinman, Phys. Rev. B **18**, 1270 (1978).
⁶⁶R. Souda and M. Aono, Nucl. Instrum. Methods B **15**, 114 (1986).
⁶⁷E. O. Kane, Phys. Rev. **159**, 624 (1967).
⁶⁸E. Wimmer, A. J. Freeman, and H. Krakauer, Phys. Rev. B **30**, 3113 (1984).
⁶⁹N. D. Lang and W. Kohn, Phys. Rev. B **7**, 3541 (1973).